General Disclaimer

One or more of the Following Statements may affect this Document

- This document has been reproduced from the best copy furnished by the organizational source. It is being released in the interest of making available as much information as possible.

- This document may contain data, which exceeds the sheet parameters. It was furnished in this condition by the organizational source and is the best copy available.

- This document may contain tone-on-tone or color graphs, charts and/or pictures, which have been reproduced in black and white.

- This document is paginated as submitted by the original source.

- Portions of this document are not fully legible due to the historical nature of some of the material. However, it is the best reproduction available from the original submission.

NF

NASA Technical Memorandum 81339

A Numerical Method for Solving the Vlasov Equation

Nobuyuki Satofuka and Koji Morinishi

February 1982

National Aeronautics and
Space Administration

NASA Technical Memorandum 81339

A Numerical Method for Solving the Vlasov Equation

Nobuyuki Satofuka, Ames Research Center, Moffett Field, California
Koji Morinishi, Kyoto Technical University, Kyoto, Japan

National Aeronautics and
Space Administration

Ames Research Center
Moffett Field, California 94035

A NUMERICAL METHOD FOR SOLVING THE VLASOV EQUATION

Nobuyuki Satofuka*
Ames Research Center, Moffett Field, California 94035

Koji Morinishi
Department of Mechanical Engineering, Kyoto Technical University
Matsugasaki, Sakyo-ku, Kyoto 606, Japan

ABSTRACT

A numerical procedure is derived for the solution of the Vlasov-Poisson system of equations in two phase-space variables. Derivatives with respect to the phase-space variables are approximated by a weighted sum of the values of the distribution function at properly chosen neighboring points. The resulting set of ordinary differential equations is then solved by using an appropriate time-integration scheme. The accuracy of the proposed method is tested with some simple model problems. The results for the free-streaming case, linear Landau damping, and nonlinear Landau damping are investigated and compared with those of the splitting scheme. The proposed method is found to be very accurate and efficient.

1. INTRODUCTION

It is well known that the Vlasov equation adequately describes the nonlinear evolution of collisionless plasmas. Since knowledge of the nonlinear behavior of plasmas in two and three dimensions is indispensable in understanding the plasma physics of controlled thermonuclear fusion, the numerical integration of the Vlasov equation has been studied intensely during recent years (refs. 1-13). However, little progress has been made on the development of fast and accurate integration schemes for the Vlasov equation in two and three dimensions for a magnetized plasma. A splitting scheme by Cheng and Knorr (ref. 12), in which the Vlasov equation is integrated in the original phase space by splitting the convective and acceleration terms in such a way that the overall scheme is second-order accurate in Δt, has been successfully applied and is one of the most promising schemes today. In two and three dimensions, however, the interpolation methods used in the scheme become more and more complicated and time-consuming, especially for magnetized plasmas (refs. 13 and 14). Development of new, accurate and efficient methods is still needed before the Vlasov equation can be solved for three-dimensional magnetized plasmas in reasonable computation time.

In this paper a new numerical method called the Modified Differential Quadrature (M.D.Q.) method, is proposed to integrate the Vlasov equation. The new method is an extension of the Differential Quadrature (D.Q.) method proposed by Bellman et al. (ref. 15). In the present method, derivatives of the distribution function with respect to the phase-space variables are approximated by a weighted sum of the values of the distribution function at properly chosen neighboring points to generate a set of ordinary differential equations in time, whereas in the original D.Q. method, these are approximated by using values at all mesh points in the computational domain.

---

*NRC-NASA Associate

As a result, computational efficiency is significantly improved with the M.D.Q. method. By changing the weighting coefficients, the spatial derivatives can easily be approximated with as much accuracy as desired. The resulting set of ordinary differential equations is then integrated by using an appropriate time-integration scheme. This solution process gives a very accurate and flexible method which is simple and straightforward to program. The present method has the feature that it is accurate to arbitrary order in space by changing the weighting coefficients and s[illegible] in time by choosing a suitable time-integration scheme. Although in this paper, the method is presented only in one dimension in order to illustrate its basic elements clearly, its extension to two and three dimensions is straightforward.

Section 2 describes the M.D.Q. method for the Vlasov equation and Section 3 describes the procedure for determining the weighting coefficients. In Section 4 we demonstrate the accuracy and efficiency of the present method through numerical experiments on simple model problems. In Section 5 we present the numerical results obtained for the free-streaming case, linear Landau damping, and nonlinear Landau damping. These results are then compared with those obtained by the splitting scheme. Section 6 presents the conclusions.

2. MODIFIED DIFFERENTIAL QUADRATURE METHOD

The system of equations under consideration consists of the one-dimensional Vlasov equation for the electron distribution function $f(x,v,t)$

$$\frac{\partial f}{\partial t} + v \frac{\partial f}{\partial x} - E \frac{\partial f}{\partial v} = 0 \tag{1}$$

and Poisson's equation for the electric field E

$$\frac{\partial E}{\partial x} = 1 - \int_{-\infty}^{\infty} f \, dv \tag{2}$$

These equations are written in dimensionless form. The basic units of time t and velocity v are the reciprocals of the so-called electron plasma frequency ω_p and the electron mean thermal velocity v_t, respectively. The distance x is measured in units of the Debye length λ_D. A periodic boundary condition in x is assumed. A rectangular mesh will be used to represent the x-v phase space with the computational domain $R = \{(x,v) | 0 \le x \le L, \ |v| \le V_{max}\}$, giving the set of points $(i\Delta x, j\Delta v) \in R$ where L is the spatial periodic length and V_{max} is the cutoff velocity, while $i = N$ and $j = 2M$ designate the number of mesh points used along the coordinates x and v, respectively.

If the distribution function f satisfying Eq. (1) is sufficiently smooth, we can write the approximate relations

$$\frac{\partial f(i,j)}{\partial x} \cong \sum_{k=1}^{N} a_{ik} f(k,j) , \qquad i = 1,2, \ldots N \tag{3a}$$

$$\frac{\partial f(i,j)}{\partial v} \cong \sum_{k=1}^{2M} a_{jk} f(i,k) \quad , \quad j = 1,2, \ldots 2M \tag{3b}$$

where index i stands for x_i, and j for v_j. In this paper we have modified the approximate relations, Eqs. (3a) and (3b), to use the values of f at the nearest N_p and M_p mesh points centered around x_i and v_j, respectively, instead of using those at all mesh points in the computational domain, as is the case in the original D.Q. method (ref. 15). By doing this, the number of arithmetic operations to be performed for every point is significantly reduced and, moreover, in the case of a uniform mesh, the weighting coefficients a_{ik} and a_{jk} become independent of the indices i and j. Therefore, the approximate relations, Eqs. (3a) and (3b), can be written as

$$\frac{\partial f(i,j)}{\partial x} \cong \sum_{k=1}^{N_p} a_k f(i + k - \alpha, j) \tag{4a}$$

$$\frac{\partial f(i,j)}{\partial v} \cong \sum_{k=1}^{M_p} a_k f(i, j + k - \beta) \tag{4b}$$

where $a_k = a_{\alpha k}$, $\alpha = (N_p + 1)/2$ in Eq. (4a) and $a_k = a_{\beta k}$, $\beta = (M_p + 1)/2$ in Eq. (4b), respectively.

Substitution of Eqs. (4a) and (4b) into Eq. (1) yields the set of Nx2M ordinary differential equations in time

$$\frac{df(i,j)}{dt} = F\left(x_i, v_j \, , \sum_{k=1}^{N_p} a_k f(i + k - \alpha, j), \sum_{k=1}^{M_p} a_k f(i, j + k - \beta), E(f), t\right) \tag{5}$$

The numerical solution of such a system, Eq. (5), is a simple task using a standard scheme for ordinary differential equations. In the present paper, we tested three schemes, namely, leapfrog, corrected leapfrog, and Stetter's method (ref. 16). All of these schemes are second-order accurate in time. As applied to Eq. (5), the schemes take the following forms:

1) leapfrog

$$f^{n+1} = f^{n-1} + 2\Delta t F^n \tag{6}$$

2) corrected leapfrog

$$\left.\begin{aligned} \overline{f^{n+1}} &= f^{n-1} + 2\Delta t F^n \\ f^{n+1} &= f^n + \Delta t(F^n + \overline{F^{n+1}})/2 \end{aligned}\right\} \tag{7}$$

3) Stetter's

$$\left.\begin{aligned} f^{(0)} &= f^n + \Delta t F^n \\ f^{(1)} &= f^n + \Delta t (F^{(0)} + F^n)/2 \\ f^{(2)} &= f^n + \Delta t (F^{(1)} + F^n)/2 \\ f^{n+1} &= \theta f^{(1)} + (1-\theta) f^{(2)} , \qquad 0 < \theta < 1 \end{aligned}\right\} \tag{8}$$

where the superscripts n and n+1 refer to time t and t+Δt, respectively, and the subscripts i and j are omitted. The electric field E is computed by a standard direct Poisson solver technique from f by Eq. (2).

3. DETERMINATION OF WEIGHTING COEFFICIENTS

In order to appropriately determine the weighting coefficients in the approximate relations, Eqs. (3a) and (3b), the test function is taken to be the following form, by analogy with Lagrange's interpolation formula,

$$p_k(x) = P(x)/[(x - x_k)P'(x_k)] \tag{9}$$

where $P(x)$ is a polynomial of degree N

$$P(x) = (x - x_1)(x - x_2) \ldots (x - x_N) \tag{10}$$

It follows that $p_k(x)$ is a polynomial of degree $N-1$ such that $p_k(x_i) = \delta_{ki}$ and $P(x_i) = 0$. If the values of a function $g(x)$ are known at N mesh points $x = x_1, x_2, \ldots x_N$, the polynomial of degree $N-1$, $\tilde{g}(x)$, which coincides with $g(x)$ at these collocation points can be written as

$$\tilde{g}(x) = \sum_{k=1}^{N} p_k(x) g(x_k) \tag{11}$$

By differentiating Eq. (11) with respect to x, we have the relation

$$\tilde{g}'(x) = \sum_{k=1}^{N} p_k'(x) g(x_k) \tag{12}$$

Using the fact that such a relation as Eq. (3a) is to be exact for $f(x) = p_k(x)$, we see that

$$a_{ik} = P'(x_i)/[(x_i - x_k)P'(x_k)] , \qquad i \neq k \tag{13}$$

For the case $i = k$, use of l'Hospital's rule gives

$$a_{kk} = P''(x_k)/[2P'(x_k)] \tag{14}$$

In their D.Q. method, Bellman et al. have chosen as P(x) the shifted Legendre polynomial of degree N, $P_N^*(x)$, selecting x_i to be the roots of $P_N^*(x)$ and determining a_{ik} explicitly (ref. 15). In this paper, as described in the previous section, we have modified the approximate relations to make use of appropriately chosen neighboring points instead of using those at all mesh points, and have adopted a uniform mesh spacing to make the weighting coefficients a_{ik} independent of index i. The weighting coefficients a_k are computed and stored once and for all at the beginning of the calculation.

4. NUMERICAL RESULTS FOR MODEL PROBLEMS

Before application to the Vlasov equation, the present method was applied to some simple model problems to demonstrate its accuracy and efficiency. First we checked the effects of the order of approximation to spatial derivatives on the accuracy of computed results. Using the test function of the form

$$f = 1 + A \cos mx \tag{15}$$

in which $A = m = 0.5$, we calculated $\partial f/\partial x$ by the approximate relation, Eq. (4a), for several values of N_p. The spatial computational domain was of periodic length $L = 4\pi$, and the total number of mesh points N was 16. The results are displayed in Table 1 in which the error is defined to be

$$\text{ERROR} = \left(\sum_{i=1}^{N} D_i^2 \Big/ N \right)^{1/2} \tag{16}$$

where D_i is the difference between the analytic solution and the numerical solution at the mesh point x_i. In Table 1 we can see that as N_p increases, the error decreases significantly, as expected. In particular, the error for $N_p = 7$ is at least 3 orders of magnitude smaller than for $N_p = 3$, while the difference between $N_p = 11$ and $N_p = 15$ is negligible due to the accumulation of roundoff errors in 32-bit, single-precision arithmetic.

The present method was then applied to the following simple linear model equation

$$\frac{\partial f}{\partial t} + c \frac{\partial f}{\partial x} = 0 \tag{17}$$

with $c = \pi/4$. The initial condition was

$$f(x,0) = 1 + A \cos mx \tag{18}$$

with $A = m = 0.5$. The analytic solution of Eq. (17) is known to be

$$f(x,t) = 1 + A \cos m(x - ct) \tag{19}$$

which gives a means of checking the accuracy of the numerical results. The computational conditions are the same as for Eq. (15).

Results are presented for two measures of the accuracy. One is $F(0.5)$, the fundamental cosine mode of f at time t, defined as

$$F(0.5) = \frac{1}{L} \int_0^L f \cos mx \, dx$$

and the other is the L_2 error of f defined by Eq. (16). Both are shown in Figs. 1-3 for the period from $t = 32$ to $t = 48$. The analytical solution for $F(0.5)$ is shown as a solid line, and the numerical solutions by symbols. The L_2 errors of f from the numerical solutions are also shown by symbols with the scale along the right ordinate.

Figure 1 compares the results obtained with $N_p = 15$ for three different time-integration schemes described in Section 2. Although the three schemes produce virtually the same results for $F(0.5)$, Stetter's scheme gives the most accurate result for L_2 error. Therefore, we decided to adopt Stetter's scheme as the standard time-integration scheme hereafter in this paper. The results with $N_p = 3$, 7, 11, and 15 are compared in Fig. 2, which shows the effects of order of approximation to the spatial derivatives. Figure 2(a) shows the results for $N_p = 7$, 11, and 15; no significant difference can be seen for $F(0.5)$, while L_2 error tends to decrease as N_p increases. The difference between $N_p = 11$ and $N_p = 15$ is again negligible due to the roundoff errors. Figure 2(b) shows results for the case of $N_p = 3$, which corresponds to the usual second-order, centered, finite-difference approximation to $\partial f/\partial x$. In this case the result for $F(0.5)$ shows a large phase error from the analytic solution, which shows the need for using a higher-order approximation for spatial derivatives. The results of the present method with $N_p = 15$, Stetter's time-integration scheme, and those of the splitting scheme of Cheng and Knorr (ref. 12) are shown in Figs. 3(a) and 3(b). Although the curves for $F(0.5)$ obtained by the two methods agree very well with the analytic solution, the L_2 error of the present method is much smaller than that of the splitting scheme.

5. RESULTS FOR THE VLASOV EQUATION

In this section we will present the results of integrating the one-dimensional Vlasov equation and demonstrate the accuracy and efficiency of the present method. As described in Section 2, we will use a rectangular mesh to represent the x-v phase space with the computational domain $R = \{(x,v) | 0 \le x < L, |v| \le V_{max}\}$. Throughout the following examples, the cutoff velocity, V_{max}, is taken to be 5.0. The symbols N and 2M designate the number of mesh points used along the x and v coordinates, respectively, while N_p and M_p denote the degree of M.D.Q. in each direction, corresponding to $N_p - 1$ and $M_p - 1$ order of accuracy, respectively.

In the first example we show results for the free-streaming case with $E(x,t) = 0$ in Eq. (1). The initial condition is

$$f(x,v,0) = f_0(v)(1 + A \cos mx) \tag{20}$$

with $A = m = 0.5$ and $f_0(v) = (2\pi)^{-1/2}\exp(-v^2/2)$. The analytic solution corresponding to this initial condition is given by

$$f(x,v,t) = f_0(v)\left[1 + A \cos m(x - vt)\right] \tag{21}$$

Here we define the density as

$$\rho(x,t) = \int_{-\infty}^{\infty} f(x,v,t)dv \tag{22}$$

Equation (21) combined with Eq. (22) leads to the following expression for the density

$$\rho(x,t) = 1 + \exp(-m^2t^2/2)A \cos mx \tag{23}$$

Numerical calculation of Eq. (22), on the other hand, gives the following expression for the density

$$\rho(x,t) = \Delta v \sum_{j=1}^{2M} f_0(v_j)\left[1 + A \cos m(x-v_jt)\right] \tag{24}$$

The numerical results are shown in Fig. 4 where the computed densities at $x = 0$ (curve A) and $x = L/8$ (curve B) are plotted against time. As can be predicted from Eq. (23), $\rho \to 1$ as $t \to \infty$, and the curves in Fig. 4 tend asymptotically to 1. The right-hand side of Eq. (24) is the sum of periodic functions of time, which results in a quasi-periodic behavior for $\rho(x,t)$ called recurrence. In the present calculation with $A = m = 0.5$, $V_{max} = 5.0$, $N = 8$, and $M = 20$, the predicted recurrence time is $T_R = 2\pi/(m\Delta v) = 49.00$. The numerical results presented in Fig. 4 agree very well with this value.

The second example shown in Fig. 5 tests linear Landau damping for the same initial condition as Eq. (20), but in this case, the electric field E is retained in Eq. (1). We used $A = 0.01$, $m = 0.5$, $N = 8$, $M = 20$, and $\Delta t = 1/8$. The abscissa is the time nondimensionalized by ω_p^{-1} and the ordinate shows the first Fourier mode $E(0.5)$ of the electric field E. The solid curve in Fig. 5 has been obtained by the present method with $N_p = 7$, $M_p = 7$, and Stetter's scheme for time integration, while the dashed curve has been obtained by the splitting scheme. In this case the electric field decays exponentially and agreement of the numerical results with Landau's theory is quite good up to $t \approx 40\ \omega_p^{-1}$, except for a slight deviation in the dashed curve shortly after $t \approx 32\ \omega_p^{-1}$. The recurrence effect occurs at

$t = 46.63\ \omega_p^{-1}$ in the present method and at $t = 46.50\ \omega_p^{-1}$ in the splitting scheme, and the times are comparable to the theoretical value $T_r = 49.00$ obtained for the free-streaming case.

The third example tests nonlinear Landau damping. The effect of a strong nonlinear perturbation, $A = 0.5$, is shown in Fig. 6 for $m = 0.5$, in which the evolution of the first three Fourier modes of the electric field E is shown. This problem has been solved by many authors (refs. 6, 10, and 12) and, therefore, is appropriate for evaluating the present method. We used $N = 16$, $M = 64$, and $\Delta t = 1/8$. The solid curve and the dashed curve in the figure show the results of the present method and the splitting method, respectively. In this case we used the present method with $N_p = 15$ and $M_p = 7$. Initially, the first mode damps much more than predicted by the linear theory while the second and third modes damp much less than Landau's theory. After $t = 15\ \omega_p^{-1}$ all modes grow exponentially until $t = 40\ \omega_p^{-1}$, where saturation occurs. The results of the first and second Fourier modes obtained by the present method are both qualitatively and quantitatively equal to the results obtained by the splitting scheme, except for a slight difference after $t \simeq 50\ \omega_p^{-1}$. For the third mode, the results show considerable differences between $t = 10\ \omega_p^{-1}$ and $t = 30\ \omega_p^{-1}$. We can see, however, that the overall behavior of the three Fourier modes by the present method is still the same as that of the splitting scheme.

With the mesh points used in this case, total time of execution (CPU time) was 55 sec using a Fujitsu FACOM M-200 computer. In order to demonstrate the accuracy and efficiency of the present method, we compare the results obtained by the present method with those of the splitting scheme with twice as many mesh points in each direction. In the former method we used $N = 16$ and $M = 64$, while in the latter, $N = 32$ and $M = 128$. The initial conditions as well as the other parameters are the same as in Fig. 6. The time evolution of the first Fourier mode of the electric field, $E(0.5)$, is plotted in Fig. 7, in which the solid curve shows the result of the present method and the dashed curve shows that of the splitting scheme. Although the difference between the two curves at times later than $t = 50\ \omega_p^{-1}$ is slightly larger than that noted in Fig. 6, the agreement can be judged as excellent. Actually the difference in Fig. 7 is much less than that existing between the splitting method itself with $N = 16$, $M = 64$, and $N = 32$, $M = 128$. We can see from Fig. 7 that with the present method, results with nearly the same accuracy can be obtained using half the number of mesh points along each direction. Although the present method requires slightly more computation time per mesh point per time step, we can conclude that the present method is more efficient than the splitting scheme even for the one-dimensional case. For multi-dimensional cases, the present method requires less computation time than the splitting scheme with the same number of mesh points.

6. CONCLUSIONS

In the present paper we have developed a numerical procedure, based on the modified differential quadrature method, for the solution of the one-dimensional Vlasov-Poisson system of equations. The derivatives with respect to the phase-space variables in the Vlasov equation are approximated as a weighted sum of the distribution function at properly chosen neighboring points. The weighting coefficients are determined similarly to Lagrangian interpolation. As a result, the approximation to phase-space derivatives can be of arbitrary order of accuracy by changing the number of mesh points used in the approximating relations. The time integration of the distribution function is performed as in the case of ordinary differential equations.

We have shown some examples that demonstrate the accuracy of the present numerical method. The results for strong nonlinear Landau damping are in excellent agreement with those using the splitting scheme. Using half the number of mesh points in each direction, we have found that the present method is as accurate as the splitting method. The important feature is that the computation time is not only quite low, but also that accurate results can be obtained with a fewer number of mesh points due to the high accuracy of approximation to the spatial derivatives.

Although we have shown the accuracy and efficiency of the present method only in one-dimensional problems, the extension to the two- and three-dimensional Vlasov equation is simple and straightforward. Compared with the splitting scheme, the present method is more efficient in multi-dimensional problems. In fact, for the two-dimensional Vlasov equation, we have obtained accurate solutions in less computation time than the splitting scheme with the same number of mesh points. The results will be presented in a forthcoming paper.

ACKNOWLEDGMENT

The research for this paper was partially conducted while the first author was an NRC-NASA Senior Research Associate at Ames Research Center, Moffett Field, California. The authors wish to thank R. W. MacCormack for his encouragement and support.

REFERENCES

1. Armstrong, T. P.; Harding, R. C.; Knorr, G.; and Montgomery, D.: Solution of Vlasov's Equation by Transform Methods. Method in Computational Physics, vol. 9, B. Alder, S. Fernbach, and M. Rotenberg, eds., Academic Press, New York, 1970, p. 30.

2. Joyce, G.; Knorr, G.; and Meier, H. K.: Numerical Integration Methods of the Vlasov Equation. J. Comp. Phys., vol. 8, 1971, pp. 53-63.

3. Emery, M. H.; and Joyce, G.: A Comparison of the Fourier-Hermite and Power Transform Solution of the Nonlinear Vlasov Equation. J. Comp. Phys., vol. 11, 1973, pp. 493-506.

4. Denavit, J.; and Kruer, W. L.: Comparison of Numerical Solutions of the Vlasov Equation with Particle Simulations of Collisonless Plasmas. Phys. Fluids, vol. 14, 1971, pp. 1782-1791.

5. Sakanaka, P. H.; Chu, C. K.; and Marshall, T. C.: Formation of Ion-Acoustic Collisionless Shocks. Phys. Fluids, vol. 14, 1971, pp. 611-614.

6. Nuhrenberg, J.: A Difference Scheme for Vlasov's Equation. J. Appl. Math. Phys. (ZAMP), vol. 22, 1971, pp. 1057-1076.

7. Canosa, J.; Gazdag, J.; Fromm, J. E.; and Armstrong, B. H.: Electrostatic Oscillations in Plasmas with Cutoff Distributions. Phys. Fluids, vol. 15, 1972, pp. 2299-2305.

8. Canosa, J.; Gazdag, J.; and Fromm, J. E.: The Recurrence of the Initial State in the Numerical Solution of the Vlasov Equation. J. Comp. Phys., vol. 15, 1974, pp. 34-45.

9. Shoucri, M. M.; and Gagne, R. R. J.: Numerical Solution of a Two-Dimensional Vlasov Equation. J. Comp. Phys., vol. 25, 1977, pp. 94-103.

10. Gazdag, J.: Numerical Solution of the Vlasov Equation with the Accurate Space Derivative Method. J. Comp. Phys., vol. 19, 1975, pp. 77-89.

11. Gros, M.; Bertrand, P.; and Baumann, G.: Multiple Water-Bag Model and Nonlinear Plasma Oscillations: Appearance of a New Pole. J. Plasma Phys., vol. 20, 1978, pp. 465-478.

12. Cheng, C. Z.; and Knorr, G.: The Integration of the Vlasov Equation in Configuration Space. J. Comp. Phys., vol. 22, 1976, pp. 330-351.

13. Shoucri, M. M.; and Gagne, R. R. J.: Splitting Schemes for the Numerical Solution of a Two-Dimensional Vlasov Equation. J. Comp. Phys., vol. 27, 1978, pp. 315-322.

14. Cheng, C. Z.: The Integration of the Vlasov Equation for a Magnetized Plasma. J. Comp. Phys., vol. 24, 1977, pp. 348-360.

15. Bellman, R.; Kashef, B. G.; and Casti, J.: Differential Quadrature: A Technique for the Rapid Solution of Nonlinear Partial Differential Equations. J. Comp. Phys., vol. 10, 1972, pp. 40-52.

16. Stetter, H. J.: Improved Absolute Stability of Predictor-Corrector Schemes. Computing, vol. 13, 1968, pp. 286-296.

TABLE 1 L_2 ERRORS OF THE M.D.Q. METHOD WITH N_p = 3, 7, 11, and 15 for $\partial/\partial x$ OF THE FUNCTION EQ. (15)

N_p	3	7	11	15
Error	0.45087E-2	0.46223E-5	0.55815E-6	0.52457E-6

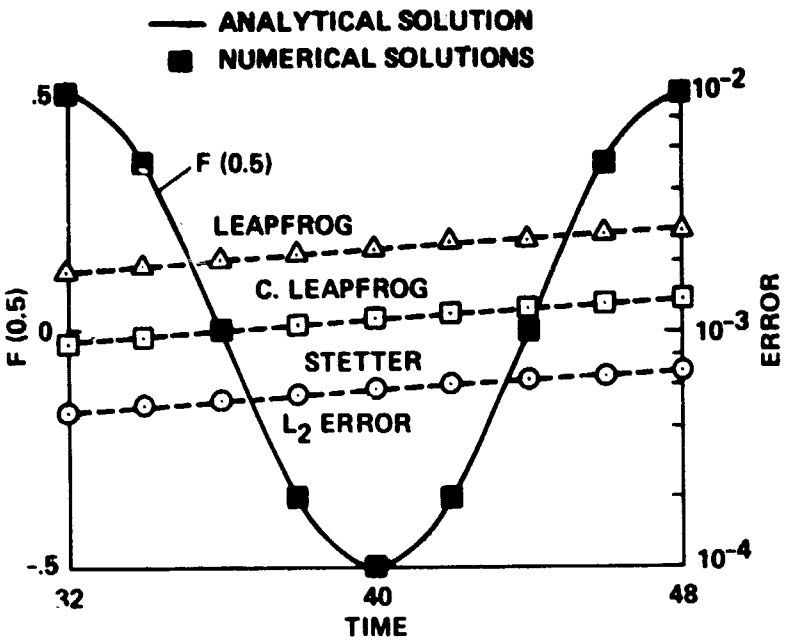

Fig. 1 Comparison of accuracy between three time-integration schemes for a linear model equation, $N_p = 15$.

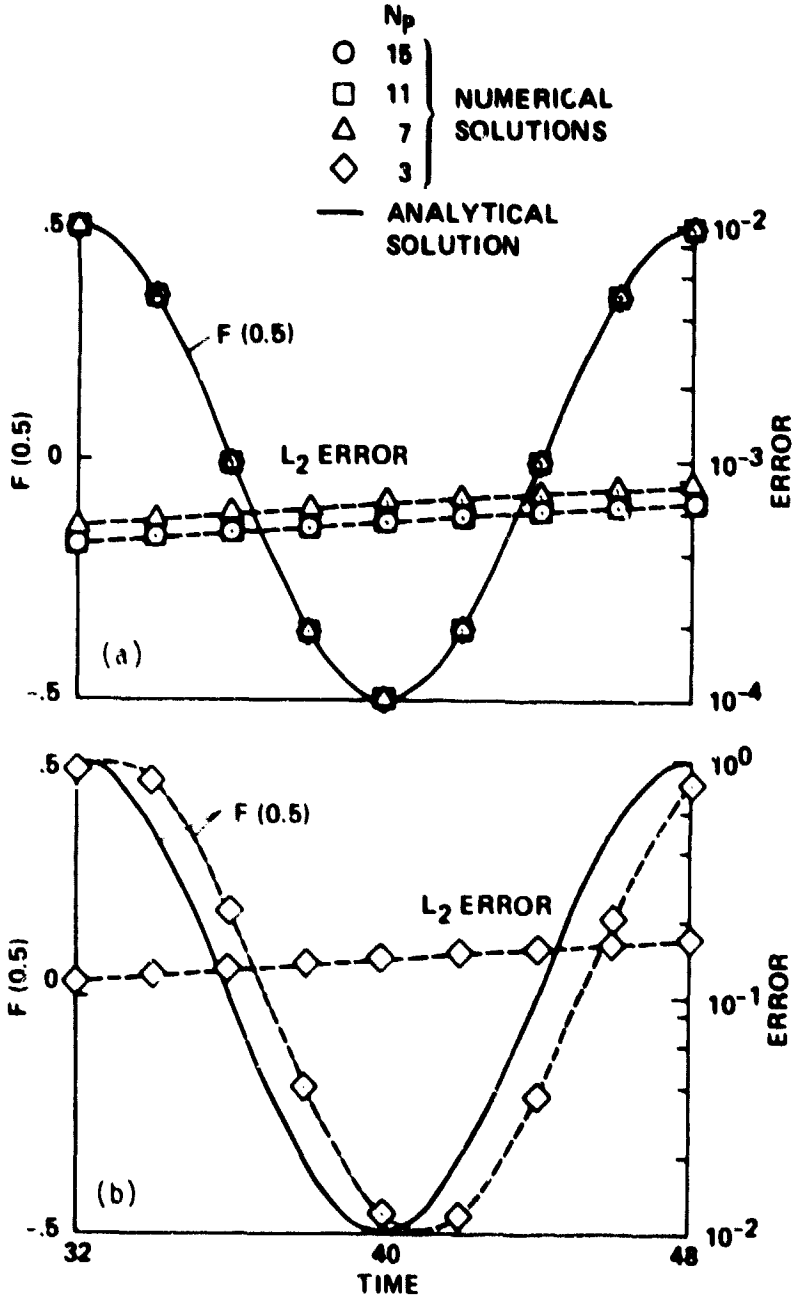

Fig. 2 Comparison of accuracy between the M.D.Q. methods with different orders of spatial approximation. (a) N_p = 7, 11, and 15; (b) N_p = 3.

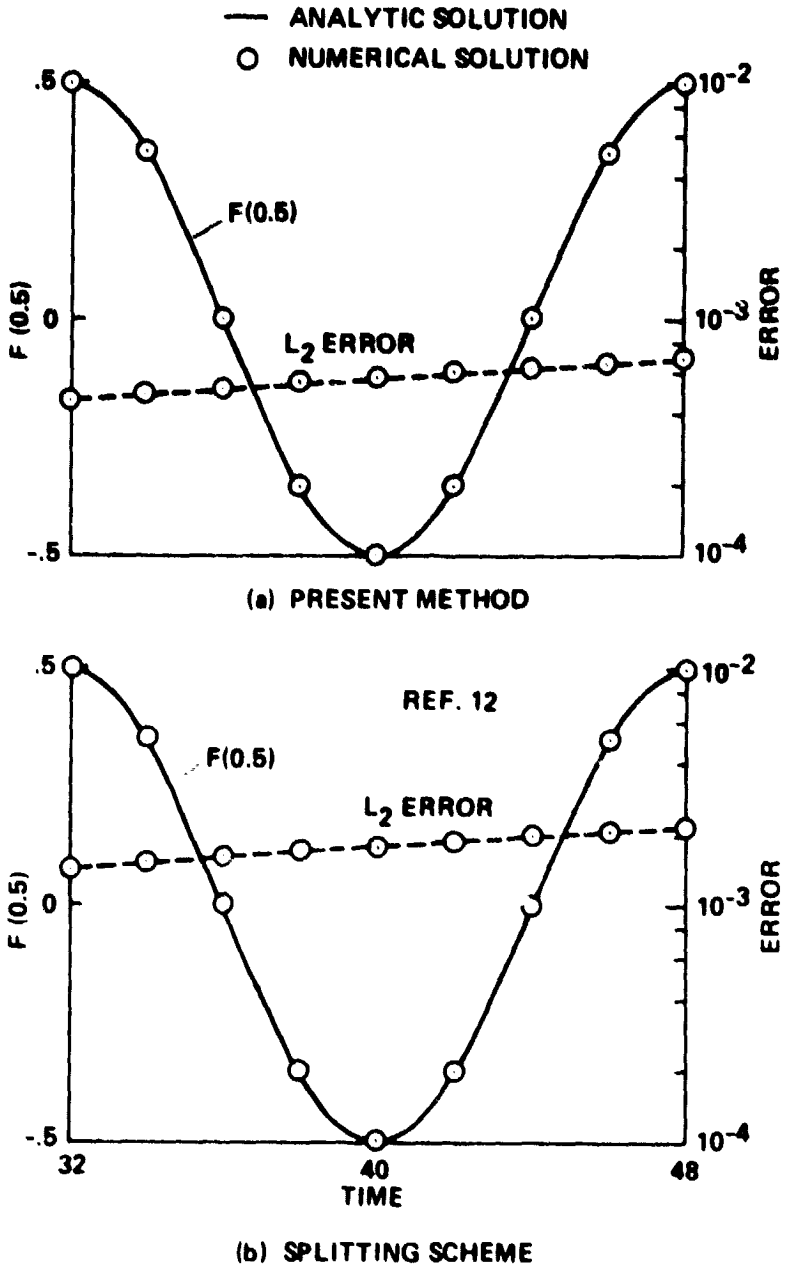

Fig. 3 Comparison of accuracy between the M.D.Q. method with N_p = 15 and the splitting scheme.

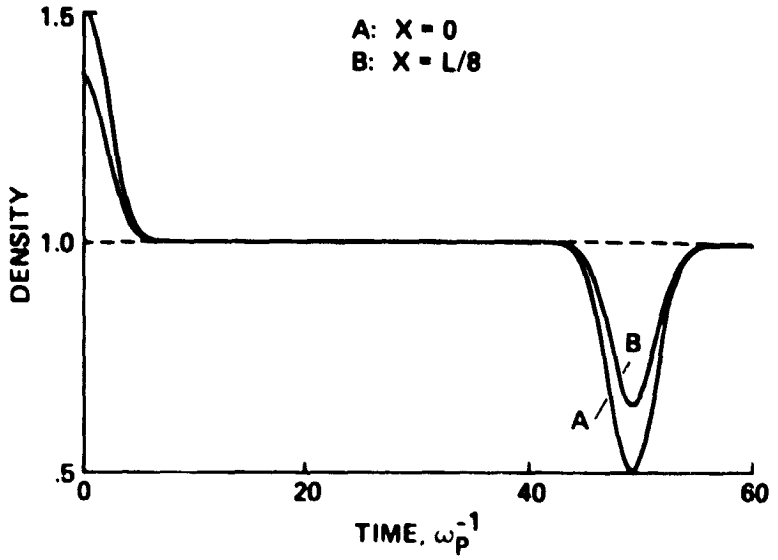

Fig. 4 Time evolution of the density at positions x = 0 (curve A) and x = L/8 (curve B), for the free-streaming case, and for the initial condition in Eq. (20). A = m = 0.5, N = 8, M = 20, N_p = 7, and Δt = 1/8.

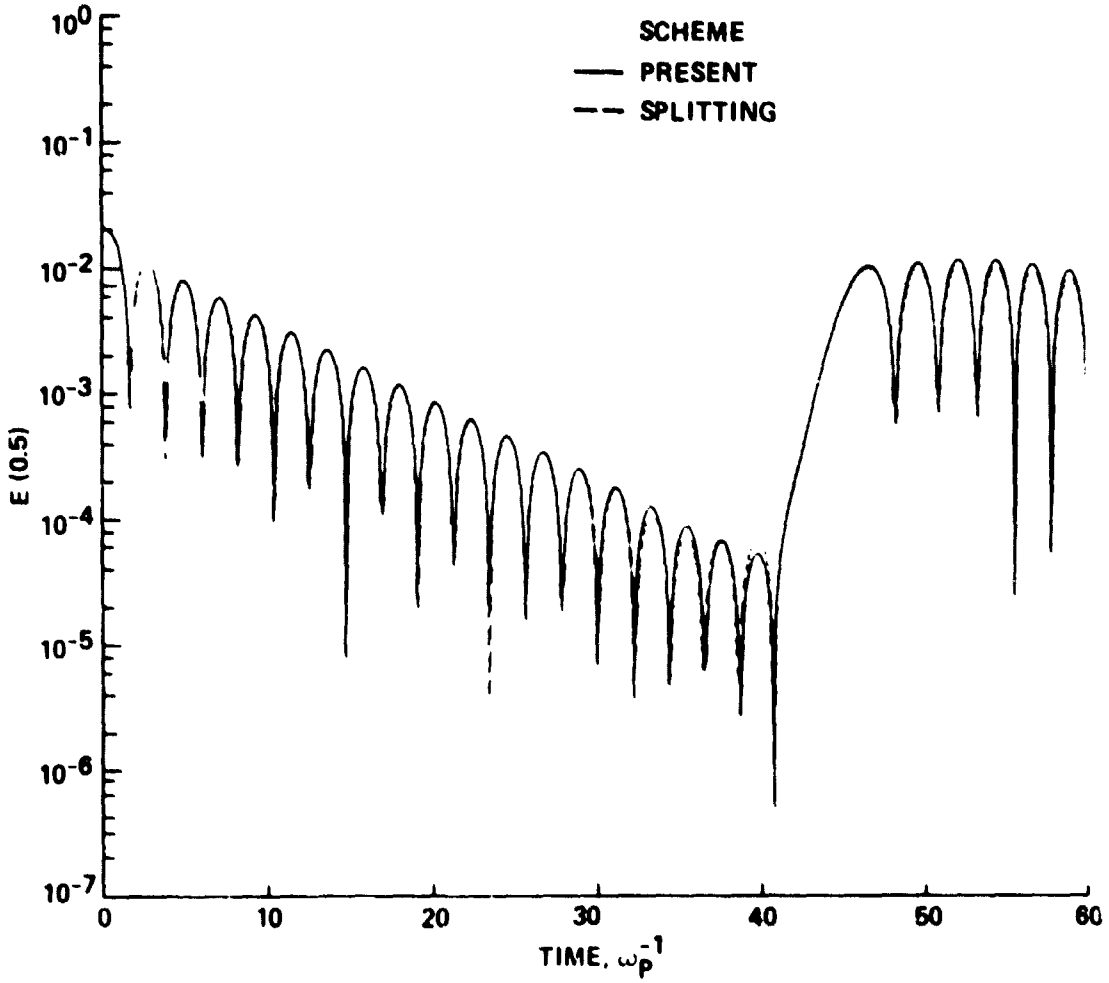

Fig. 5 Electric field vs. time for linear Landau damping with A = 0.01, m = 0.5, N = 8, M = 20, N_p = 7, M_p = 7, and Δt = 1/8.

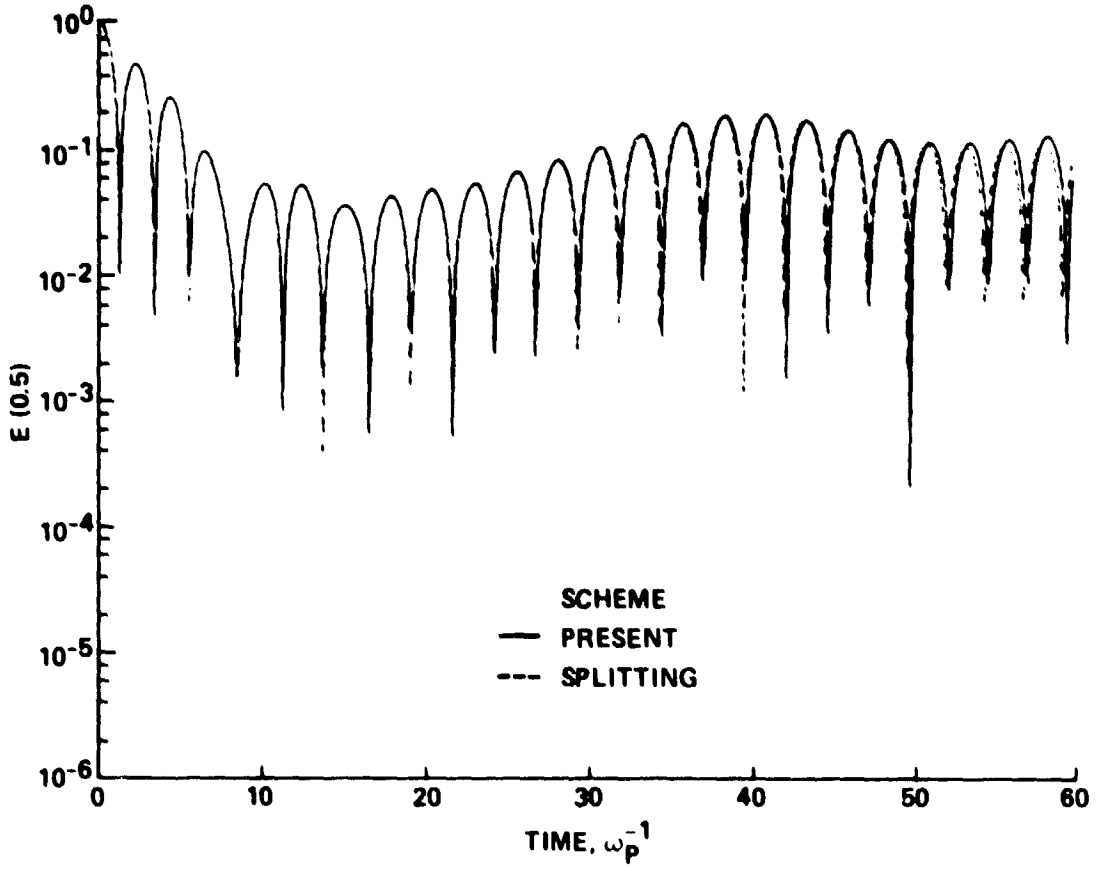

(a) First Fourier mode, E(0.5).

Fig. 6 Electric field vs. time for strong nonlinear Landau damping with A = m = 0.5, N = 16, M = 64, N_p = 15, M_p = 7, and Δt = 1/8.

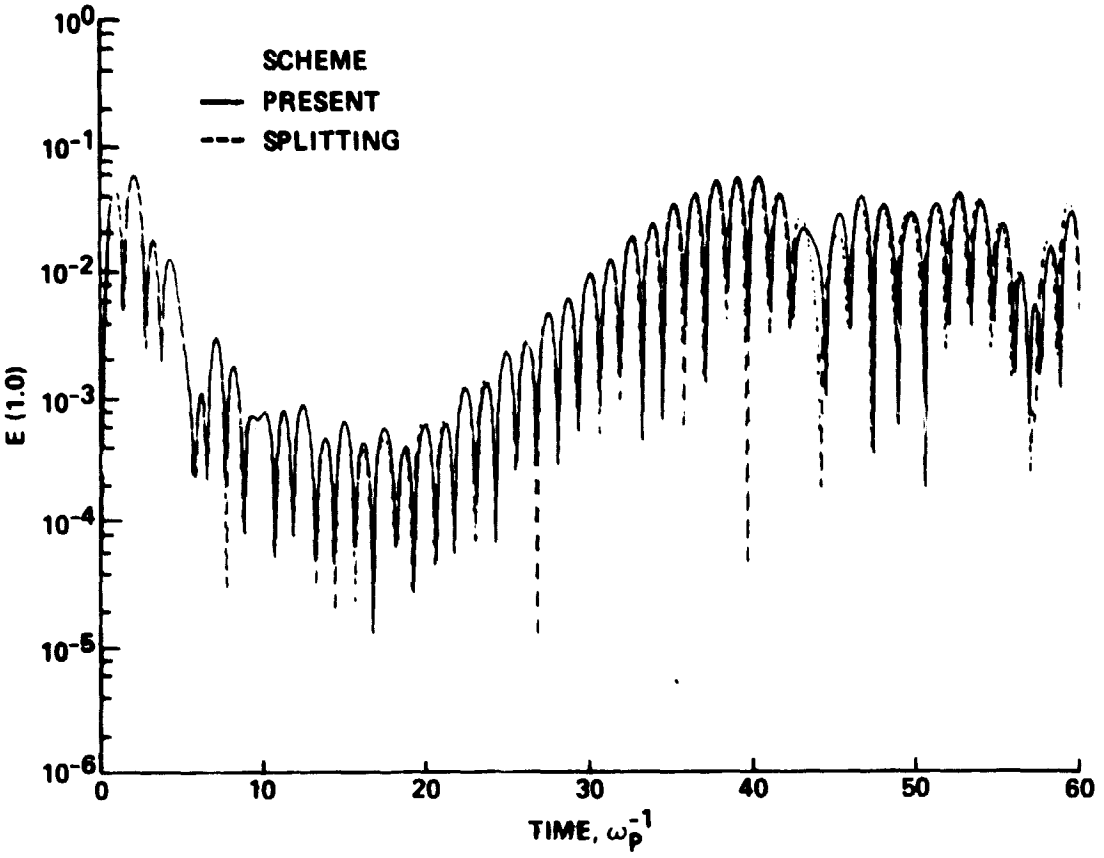

(b) Second Fourier mode, E(1.0).

Fig. 6 Continued.

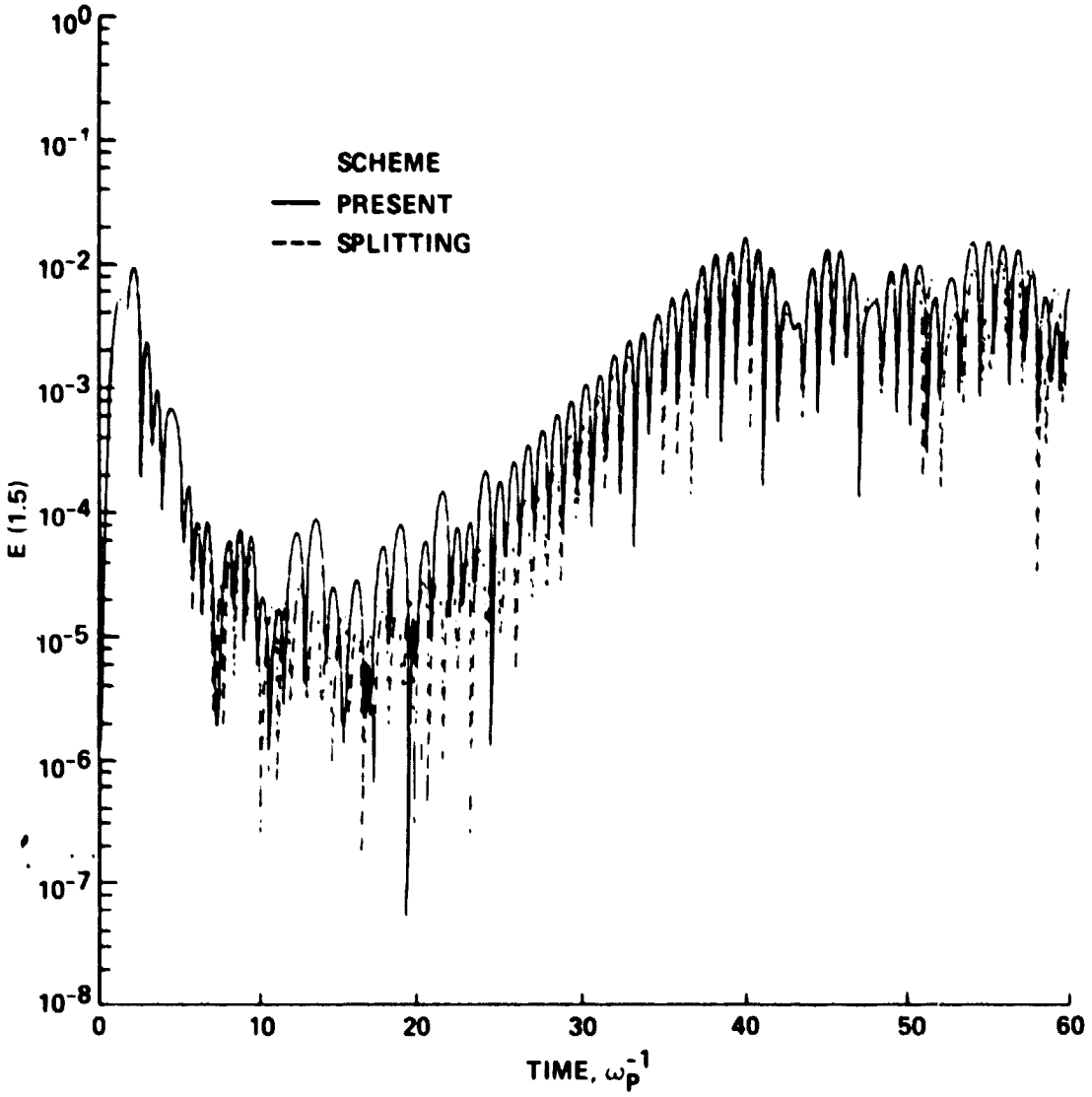

(c) Third Fourier mode, E(1.5).

Fig. 6 Concluded.

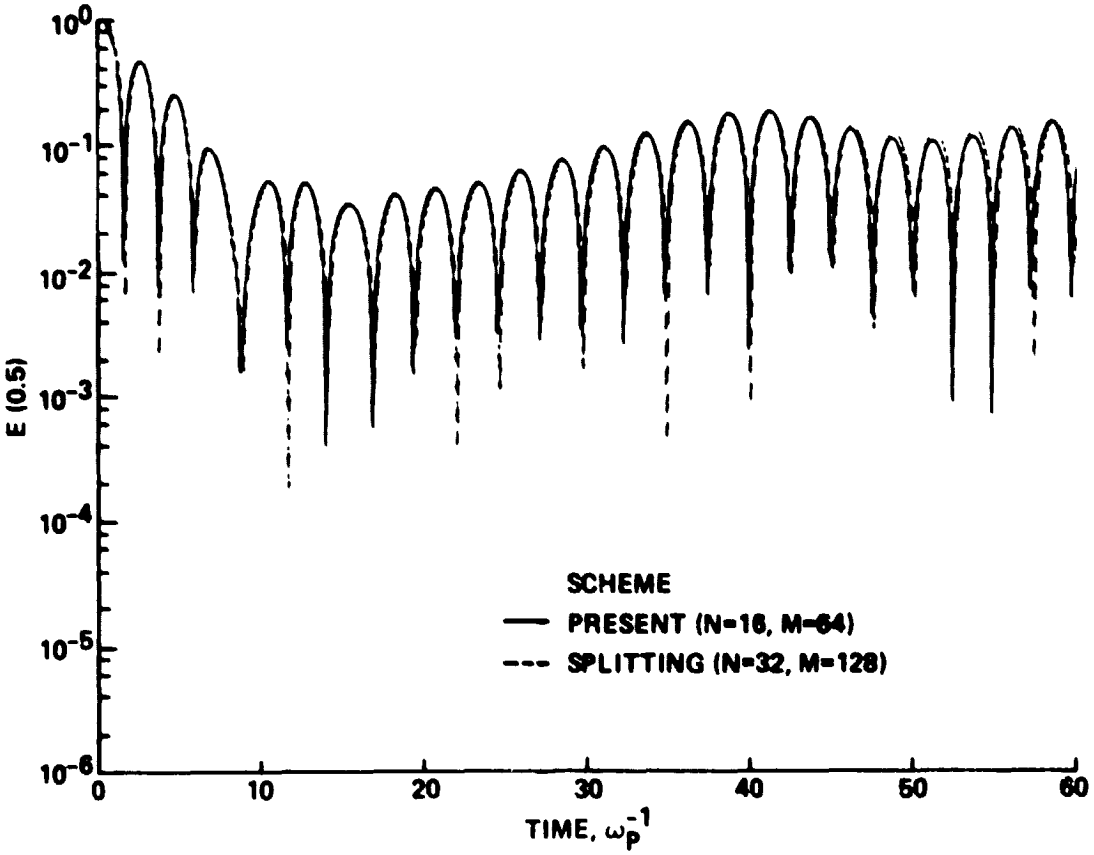

Fig. 7 Comparison of results for the first mode of electric field. Solid curve: M.D.Q. method with N = 16 and M = 64; dashed curve: splitting scheme with N = 32 and M = 128.